METHODS

Apatite (U-Th)/He dating

Multiple, large (>100 μm), inclusion-free apatite crystals were selected from each sample. Helium was extracted through heating with a Nd-YAG laser and the released gas was analysed and quantified with a mass spectrometer. Uranium and thorium contents of the same crystal were subsequently determined by single- and multiple-collector inductively-coupled plasma mass spectrometry at ETH Zürich. Further analytical details are documented in Wipf (2006). Sample details and results are given in Table DR1.

Problematic samples: Single-crystal AHe ages from samples H3 and H6 (Fig. 3, Table DR1) show a degree of scatter which is likely to be a reflection of two factors: i) slow cooling through the apatite helium partial retention zone (Wipf, 2006) and ii) uncertainties caused by factors such as zonation within individual crystals, implantation and loss of helium, and inclusions (Fitzgerald et al., 2006). Measurement of multiple grains within each sample thus indicates samples that yield apparently spurious ages. Sample H3 displays a wide range of ages from 46.1 to 102.1 Ma, likely due to observed strong compositional zonation within the crystals and/or microscopic U-bearing inclusions. Despite these inconsistencies, we include all grains from H3 to illustrate some of the potential pitfalls that may arise from not analysing multiple grains. A single crystal from sample H6 yields an age of 6.3 Ma, far less than the other three crystals from the sample. We ascribe this anomalously young age to He loss, and omit it from our model calculations.

Apatite fission-track analysis (AFT)

Details of the sample preparation and analytical procedures followed are described elsewhere (Seward, 1989; Richardson et al., 2008). Sample locations, details and results are given in Table DR2, while radial plots of all single-grain ages are given in Figure DR2. AFT forward modelling was carried out using HeFTy software (Ketcham, 2005), applying the annealing model of Ketcham et al. (1999), and correcting angles to the apatite crystallographic C-axis (Ketcham, 2003). Since this modelling method uses etch pit (Dpar) dimensions obtained by etching for 20 s in 5N HNO_3 as a kinetic parameter, and the apatites in this study were etched with 7% HNO_3 at 21˚C for 50 s, values were adjusted by a factor of 0.8 (Sobel and Seward, 2006). Temperature constraints on the forward models were derived from independent geological data. Several km of stratigraphic section ranging from Archean to Jurassic age lie both conformably and unconformably above the Huangling Granite (Ma et al., 2002). Thus the models were constrained to temperatures of 160 to 200˚C between 200 and 100 Ma to reflect burial well below the apatite partial annealing zone. Outside of this constraint, the models were free to choose the best-fit paths by fitting the distribution using the Kolmogorov-Smirnov statistical test. The initial mean track length was set at 16.3 μm. The AHe ages were not used to constrain the AFT thermal models.

REFERENCES

Fitzgerald, P.G., Baldwin, S.L., Webb, L.E., and O'Sullivan, P.B., 2006, Interpretation of (U–Th)/He single grain ages from slowly cooled crustal terranes: a case study from the Transantarctic Mountains of southern Victoria Land: Chemical Geology, v. 225, p. 91-120.

Ketcham, R.A., 2003, Observations on the relationship between crystallographic orientation and biasing in apatite fission-track measurements: American Mineralogist, v. 88, p. 817-829.

Ketcham, R.A., 2005, Forward and inverse modeling of low-temperature thermochronometry data, *in* Reiners, P.W. & Ehlers, T.A., eds., Low-temperature thermochronology: techniques, interpretations, and applications: Mineralogical Society of America Reviews in Mineralogy and Geochemistry 58, p. 275-314.

Ketcham, R.A., Donelick, R.A., and Carlson, W.D., 1999, Variability of apatite fission-track annealing kinetics III: extrapolation to geological time scales: American Mineralogist, v. 84, p. 1235-1255.

Ma, L., Qiao, X., Min, L., Fan, B., Ding, X., and Liu, N., 2002, Geological Atlas of China: Geological Publishing House, Beijing.

Richardson, N.J., Densmore, A.L., Seward, D., Wipf, M., Li, Y., Ellis, M.A., and Zhang, Y., 2008, Extraordinary denudation in the Sichuan Basin: insights from low-temperature thermochronology adjacent to the eastern margin of the Tibetan Plateau: J. Geophys. Res., v. 112, doi:10.1029/2006JB004739.

Seward, D., 1989, Cenozoic basin histories determined by fission-track dating of basement granites, South Island, New Zealand: Chemical Geology, v. 79, p. 31–48.

Sobel, E.R., and Seward, D., 2006, Influence of etching conditions on apatite fission track etch pit diameter, *in* Ventura, B., and Lisker, F., eds., European conference on thermochronology, Schriftenreihe der Deutschen Gesellschaft für Geowissenschaften 49**,** p. 128-130.

Wipf, M.A., 2006, Evolution of the Western Cordillera and coastal margin of Peru: evidence from low-temperature thermochronology and geomorphology [Ph.D. thesis]: Zürich, ETH Zürich, http://e-collection.ethbib.ethz.ch/show?type=diss&nr=16383, 152 p.

Figure Caption

Figure DR1. Radial plots of AFT data with single grain ages marked as squares, and central ages for each sample marked as a thick black line.

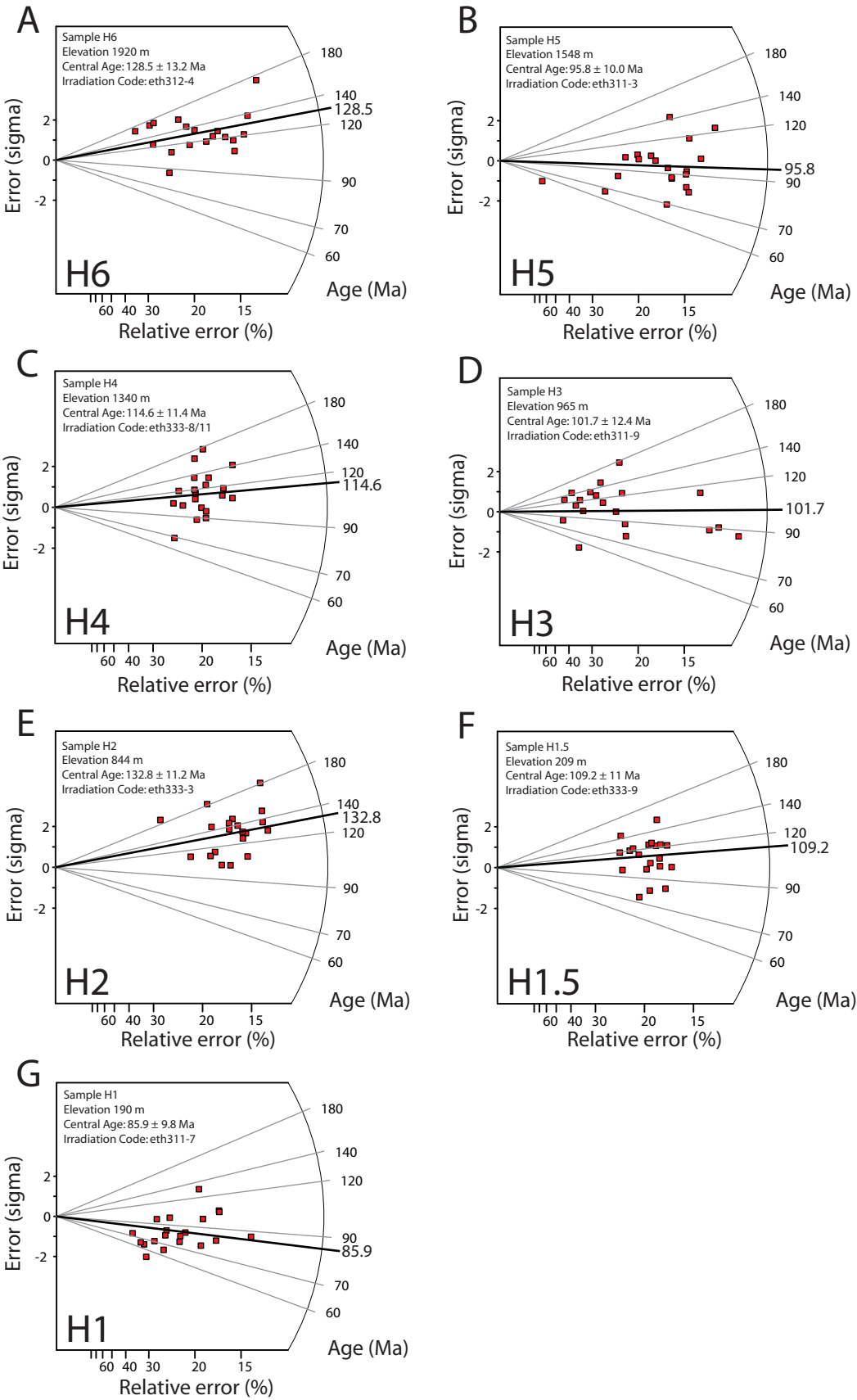
A
Sample H6
Elevation 1920 m
Central Age: 128.5 ± 13.2 Ma
Irradiation Code: eth312-4
H6
128.5
B
Sample H5
Elevation 1548 m
Central Age: 95.8 ± 10.0 Ma
Irradiation Code: eth311-3
H5
95.8
C
Sample H4
Elevation 1340 m
Central Age: 114.6 ± 11.4 Ma
Irradiation Code: eth333-8/11
H4
114.6
D
Sample H3
Elevation 965 m
Central Age: 101.7 ± 12.4 Ma
Irradiation Code: eth311-9
H3
101.7
E
Sample H2
Elevation 844 m
Central Age: 132.8 ± 11.2 Ma
Irradiation Code: eth333-3
H2
132.8
F
Sample H1.5
Elevation 209 m
Central Age: 109.2 ± 11 Ma
Irradiation Code: eth333-9
H1.5
109.2
G
Sample H1
Elevation 190 m
Central Age: 85.9 ± 9.8 Ma
Irradiation Code: eth311-7
H1
85.9
Error (sigma)
Relative error (%)
Age (Ma)
180
140
120
90
70
60
2
0
-2
60 40 30 20 15

Table DR1: Apatite (U-Th)/He data

Sample	Elevation (m)	Grain number	U (ppm)	Th (ppm)	He (nmol/g)	Grain width (μm)	Grain length (μm)	Corrected age (Ma)[*]	Mean age (Ma)[†]
H6	1923	*1*	*53.2*	*120.1*	*1.66*	*80*	*112*	*6.3 ± 0.2*	
		2	18.8	56.6	9.13	115	220	67.6 ± 0.8	
		3	29.4	86.8	13.06	88	145	72.1 ± 1.0	
		4[§]	26.9	49.6	14.61	113	238	88.8 ± 1.4	
H6		**2 to 4**							**76 ± 22**
H5	1548	1[§]	14.5	61.0	8.68	189	210	64.4 ± 1.0	
		2	32.3	142.9	14.89	121	163	53.9 ± 1.0	
		3	15.1	59.2	7.76	166	198	59.8 ± 1.0	
H5		**1 to 3**							**59 ± 11**
H4	1350	1[§]	11.3	8.1	1.90	78	172	40.8 ± 1.6	
		2[§]	9.6	9.3	2.38	88	170	52.1 ± 2.0	
		3[§]	10.7	18.5	2.35	75	220	43.2 ± 1.3	
H4		**1 to 3**							**45 ± 12**
H3	970	1	35.4	93.0	22.81	88	200	102.1 ± 0.9	
		2	8.7	27.7	6.11	133	165	97.7 ± 1.9	
		3	12.6	30.3	3.25	92	178	46.1 ± 1.4	
		4[§]	9.1	19.6	4.34	106	180	78.9 ± 2.1	
		5[§]	13.4	37.1	6.33	103	130	67.8 ± 1.6	
H3		N/A							N/A
H2	844	1[§]	25.3	47.9	5.73	85	130	41.3 ± 0.8	
		2[§]	35.8	75.6	7.79	83	135	40.4 ± 0.7	
		3[§]	19.8	38.0	4.87	100	216	42.5 ± 0.7	
H2		**1 to 3**							**41 ± 2**
H1	190	1	27.4	24.6	5.24	97	201	40.7 ± 0.5	
	190	2	22.6	23.5	4.36	96	222	42.5 ± 0.5	
	190	3[§]	20.7	18.0	5.00	83	164	55.3 ± 1.0	
H1		**1 to 3**							**46 ± 16**

Notes:

[*]Corrected ages are given as ± 2σ.

[†]Arithmetic mean ages ± 2 s.d. No mean age was calculated for sample H4 because of the large spread in single-grain ages.

[§]Denotes grains analyzed using single collector ICP-MS; all other grains analyzed using multi-collector ICP-MS (both at ETH Zürich).

Samples in italics were discarded and are not considered in further analysis.

Concentrations in ppm are based upon crystal sizes and are therefore associated with large but unknown errors.

Table DR2: Apatite fission track data

Sample	Irradiation code	Location (UTM Zone 49)	Altitude (m)	Number of grains counted	$\rho_d \times 10^5$ cm^{-2} (number counted)*	$\rho_s \times 10^5$ cm^{-2} (number counted)*	$\rho_i \times 10^5$ cm^{-2} (number counted)*	Mean track length (μm)†	P(χ^2) (% variation)§	Central age (Ma)#
H6	eth312-4	494238, 3438968	1923	20	12.02 (4809)	24.82 (931)	38.48 (1443)	14.2 ± 0.9 (101)	14 (75)	129 ± 13
H5	eth311-3	493248, 3436526	1548	20	10.26 (5224)	16.77 (1095)	29.76 (1943)	14.1 ± 1.1 (106)	24 (21)	96 ± 10
H4	eth-333-8/11	494970, 3435657	1350	20	9.99 (2641)	6.71 (838)	10.15 (1267)	n.d.	36 (8)	115 ± 11
H3	eth311-9	496930, 3422661	965	20	9.36 (5224)	8.92 (740)	13.87 (1147)	13.9± 1.1(90)	22 (27)	102 ± 12
H2	eth333-3	496665, 3428544	844	20	12.50 (2641)	13.96 (1173)	22.75 (1912)	14.1 ± 1.1 (100)	39 (6)	133 ± 11
H1.5	eth333-9	500926, 3416177	209	20	10.20 (2641)	11.89 (856)	19.90 (1434)	14.0 ± 1.2 (100)	57 (17)	109 ± 11
H1	eth311-7	500231, 3412888	190	20	9.66 (5224)	12.54 (651)	23.43 (1216)	13.6 ± 1.3 (166)	15 (70)	86 ± 10

Notes:

*ρ_d, standard track density; ρ_s, sample spontaneous track density; ρ_I, sample induced track density. Figures in parentheses are numbers of tracks counted

†Mean track lengths are c-axis corrected (Ketcham, 2003); the error represents the standard deviation of the distribution. Figures in parentheses are number of track length measurements

§P(χ^2) is the probability of χ^2 for *v* degrees of freedom, where *v* equals number of grains – 1

#Central ages are given as ± 2 s.d.

n.d.: no data. $\gamma_D = 1.55125 \times 10^{-10}$. A geometry factor of 0.5 was used. Zeta = 334 ± 9 for CN5/apatite (samples H1, H3, H5, and H6), and 350 ± 5 (samples H1.5, H2, and H4). Irradiations were performed at the ANSTO facility, Lucas Heights, Australia.